IECON 2024 - 50th Annual Conference of the IEEE Industrial Electronics Society | 978-1-6654-6454-3/24/$31.00 ©2024 IEEE | DOI: 10.1109/IECON55916.2024.10905663

Assessing Dynamic Response of MTDC Offshore-Onshore Energy Systems for Stability Enhancement in Hybrid Power Systems

Owen van Hooff , Monika Sharma, José L. Rueda Torres, Peter Palensky
Department of Electrical Sustainable Energy, TU Delft, Delft, Netherlands
{O.vanHooff@student., M.Sharma-3@, J.L.RuedaTorres@, P.Palensky@} tudelft.nl

***Abstract*—This study investigates the dynamic performance of hybrid power systems, with a focus on Multi-Terminal Direct Current (MTDC) interconnected offshore-onshore systems, under various disturbances. Conventional performance metrics such as Rate of Change of Frequency (RoCoF), commonly used for AC systems, are utilized to assess frequency response. Additionally, a modified Rate of Change of Voltage (RoCoV) metric is proposed to capture DC voltage behavior. The effectiveness of these metrics is evaluated through simulations involving various disturbances, including generator outages, line outages, converter outages, and faults. The results demonstrate the ability of the proposed metrics to effectively capture the impact of disturbances on system response, while also identifying limitations in capturing oscillating responses. Furthermore, the parametric sensitivity of control parameters in the converter's outer control loop is analyzed to assess their influence on system behavior.**

***Index Terms*—Dynamic Stability, MMC-MTDC, Offshore-Onshore Systems**

I. Introduction

The increasing integration of Renewable Energy Sources (RES) into power grids poses significant challenges in maintaining stability, particularly during disturbances. As RES penetration increases, power grids become more vulnerable to oscillations and instability, thereby threatening reliable power supply. The reliable supply of electricity is essential for modern society, and the power grid plays a critical role in ensuring this crucial service [1]. However, the integration of RES, including wind and solar power, poses significant challenges to maintain system stability, particularly during disturbances. The inherent intermittency of RES can lead to fluctuations in power generation, which can disrupt the delicate balance between supply and demand, potentially causing oscillations and instability. Multi-Terminal Direct Current (MTDC) transmission systems offer a promising solution to address these challenges by facilitating the efficient transmission of large amounts of power from offshore wind farms to onshore grids [2].

Resilience, the ability of a power system to withstand and recover from disturbances, is paramount to mitigating the societal impact of large blackouts and instability [2]. Resiliency assessment typically involves evaluating the system's performance during three distinct stages: disturbance progress, post-disturbance, and restorative. During the disturbance progress phase, the system's resilience deviates from its pre-disturbance level, and this can be assessed by monitoring various network metrics. If effective primary control actions are implemented, the system reaches a new steady-state operating condition, albeit different from the pre-disturbance state. Finally, in the restorative phase, the system recovers and returns to normal operation. Resilience assessment encompasses evaluating all three stages to gain a comprehensive understanding of the system's robustness [3]. Depending on the specific focus of the study, different technical aspects of the system may be examined [4].In recent literature [5], the impact of disturbances has been primarily assessed visually by observing the temporal variations of dynamic variables such as DC voltage magnitude and active power flow. However, evaluating the suitability of state-of-the-art performance indicators remains an open challenge. This study focuses on the assessment of the during-disturbance phase, as future power grids with limited reserves and control capabilities require a robust initial response to disturbances.

Despite the extensive research on the impact of disturbances on power grids, particularly in visual assessments of temporal variations in DC voltage magnitude and active power flow, there remains a gap in evaluating the effectiveness of performance indicators and control adjustments in MTDC-linked offshore-onshore systems. This study addresses this gap by focusing on the dynamics during disturbances and proposing performance metrics for DC side. The contributions of this paper lie in identifying the boundaries of these performance metrics with and without adjusting control parameters in the outer control loop.

The paper is structured as follows: Section II introduces the performance metrics employed to quantify the impact of disturbances. Section III describes the implemented test system, while Section IV presents the numerical results. Finally, Section V summarizes the key findings and conclusions of the study.

II. Performance Metrics

The impact of disturbances on the dynamic performance of hybrid AC/DC power systems is crucial for ensuring system stability [1]. This study introduces two performance metrics to evaluate the response of such systems to disturbances: RoCoF for the AC system and RoCoV for the DC system. These metrics provide insights into the dynamic behavior of the system and its ability to maintain stability following disturbances.

A. AC Side Metric: RoCoF

Frequency stability is a critical aspect of power systems, as it determines the synchronous operation of the system. The frequency response after a disturbance typically consists of four stages: inertia response, primary frequency control, secondary frequency control, and tertiary frequency control [6]. The first stage, known as the inertia response, is of primary interest in this study. It is characterized by a rapid drop in frequency following the disturbance, primarily due to the conversion of kinetic energy into electrical energy [7]. The larger the inertia of the system, the smaller the frequency deviation.

To quantify the inertia response, the RoCoF is commonly employed [8]. The RoCoF is defined as the derivative of frequency over time, as shown in the equation below:

$$RoCoF = \frac{|f(t_0 + T) - f(t_0)|}{T} \tag{1}$$

where $f(t)$ is the frequency at time t and T is the time window. High RoCoF values indicates the need for protection devices, e.g. Under-Frequency Load-Shedding (UFLS) [9].

B. DC Side Metric: RoCoV

In HVDC systems, voltage magnitude is the primary control parameter for power flow management. Voltage stability refers to the ability of the system to maintain voltage within permissible limits [11]. Existing voltage stability indices in the literature are primarily designed for steady-state assessment. Therefore, a new metric is needed to capture the dynamic behavior of DC voltage after disturbances.

The design of protection schemes in DC systems often utilizes the RoCoV metric [12]. It is defined similarly to RoCoF, as shown in the equation below:

$$RoCoV = \frac{|V_{DC}(t_0 + T) - V_{DC}(t_0)|}{T} \tag{2}$$

where, $V_{DC}(t)$ is the DC voltage magnitude and T is the time window of calculation. In protection schemes, T is typically set to match the measurement sampling period (in the order of milliseconds) to ensure rapid protective action. After conducting several EMT simulations, a longer time window (0.1-0.4 seconds) is considered, aligning with the typical response time of primary DC voltage control caused by an abrupt power imbalance [13].

III. Test System

The test system and all numerical simulations presented in this paper are conducted using the RSCAD® FX software version 1.3.2, running on a NovaCor 7-core 3.5 GHz chassis ([14], [15]). The CIGRE BM1 benchmark model is employed for the simulations, as shown in the single-line diagram in Figure 1. This model represents a 5-terminal bipole MTDC system, comprising 4 AC/DC terminals and 1 DC/DC terminal.

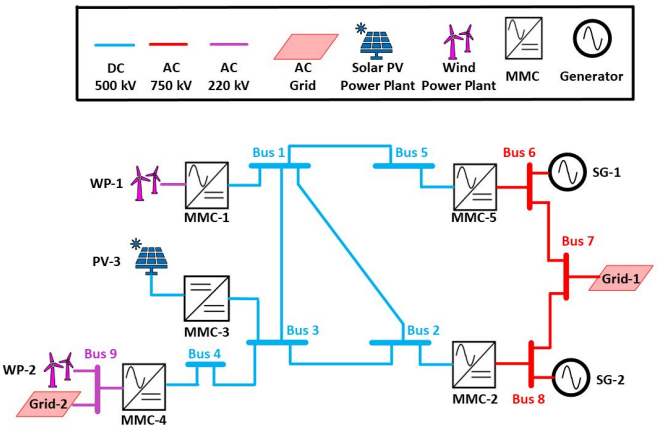

Fig. 1. Multi-terminal HVDC test system B4.72 BM1

A. Converter Model

The BM1 model comprises five converter stations, each equipped with MMC technology to convert AC voltages to DC voltages and vice versa. The simulation employs the MMC5 model from RSCAD® FX ([17]), a processor-based model that manages capacitor voltages within the simulation itself. Designed for evaluating high-level controls and system performance, the MMC5 model assumes internal balancing of capacitor voltages within each submodule ([17]). Table I provides the ratings and setpoints for the five converters.

TABLE I
Bipole Converter Setpoints and Ratings for CIGRE BM1 Model

Converter	Rating (MW)	Setting
MMC-1	2500	P = 1800 MW, $Q = 0$
MMC-2	5000	Vdc = 1 p.u., $Q = 0$
MMC-3	2500	P = -1500 MW
MMC-4	2500	P = -1500 MW, $Q = 0$
MMC-5	2500	P = 2000 MW, $Q = 0$

B. Transmission Line Model

All transmission lines and cables are modeled as frequency-dependent traveling waves. The parameters and lengths are given in Table II [16].

C. Wind Power Plant and Solar PV Power Plant Model

Wind power plants are simulated as controlled AC voltage sources behind an impedance, while solar PV power plants are modeled as controlled DC voltage sources coupled with DC/AC inverters ([16]). Their ratings and settings are included in Table III.

TABLE II
TRANSMISSION LINE DATA FOR CIGRE BM1 MODEL

Line type	DC kV ± 500	AC 750 kV	AC 220 kV
R_{ac} (Ω/km)		0.013	0.040
X_{ac} (Ω/km)		0.261	0.304
B_{ac} (S/km)		4.12e-8	1.85e-6
R_{dc} (Ω/km)	0.0062		
Max Current (kA)	5.0	5.27	1.76

TABLE III
POWER PLANT PARAMETERS FOR CIGRE BM1 MODEL

Name	Rating (MW)	Setting (MW)
SG-1	3000	3000
SG-2	3000	2000
WP-1	2500	1800
WP-2	2500	1600
PV-3	2500	1500

D. Control System Design

A master-slave hierarchical control is used within the DC side. MMC-2 performs DC voltage control, whereas the other MMCs perform active power control. Table IV shows the control parameters of the outer control loop [18].

TABLE IV
OUTER LOOP PARAMETERS

	DC voltage	Active power	AC voltage	Reactive power
K_p	14 p.u.	0	1 p.u.	1 p.u.
Ki	0.2 s	0.0303 s	0.1 s	0.0303 s
DBS		14 p.u.		
DBW		5 %		

IV. NUMERICAL RESULTS

A. Disturbance Analyses

The system's resilience to various component outages is evaluated, including converter, generator, and line failures. The impact of these outages on DC voltage and frequency is further assessed.

1) Outages: Figure 2 illustrates the DC voltage response at bus 5 for different outages. The Outages at MMC-2 and DC line 1-2 exhibit minimal impact on DC voltage stability. However, outages of MMC-5 or DC line 1-5 resulted in substantial voltage dips, indicating a higher susceptibility to these outages. This is attributed to the larger power imbalances induced by these outages, which the DC network struggled to compensate for.

Fig. 2 also illustrates the collateral effect on the DC voltage response at bus 5 due to outages at the AC side of the network. Loss of SG-2, affects the DC voltage performance due to power imbalances. The loss of SG-2, particularly, causes significant and oscillatory voltage deviations as depicted in Fig. 3. This is because SG-2 is located near MMC-2, which plays a crucial role in DC voltage regulation. The loss of SG-2 disrupted power balancing at MMC-2, hindering its ability to maintain stable DC voltage. Fig. 4 shows the propagation of the oscillations in line 1-2 across line 1-5.

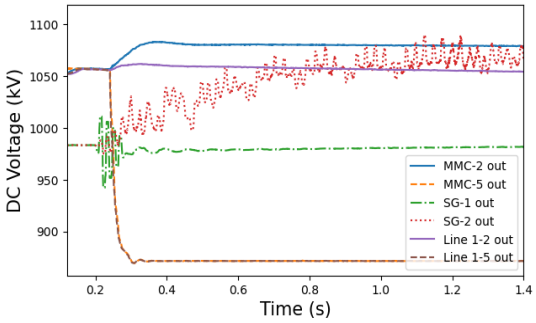

Fig. 2. DC voltage response at bus 5 for different outages

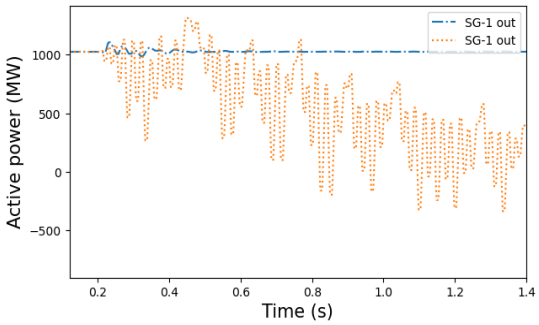

Fig. 3. Active power flow in line 1-2 for different outages

.

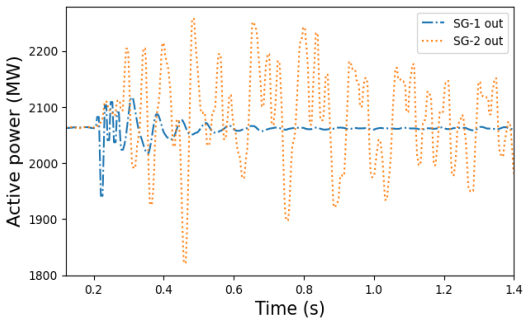

Fig. 4. Active power flow in line 1-5 for different outages

The loss of any synchronous generator led to noticeable frequency excursions. In Fig. 5, the frequency response at bus 7 under different outages is shown. SG-2 loss have the most severe impact, as it reduces the control response of MMC-2. This triggered active power oscillations at the DC side, which propagated back to the AC side through MMC-5, exacerbating frequency instability as depicted in Fig. 6.

2) Short Circuits: The dynamic behavior of the DC voltage at bus 5 was evaluated under different short circuit scenarios, both on the AC and DC sides of the system. The results revealed that AC side short circuits resulted in transient overshoots within 10 % of the nominal voltage, followed by a gradual recovery. Conversely, DC side short circuits triggered severe voltage dips with steep slopes. The most severe case involved a line-to-line fault near an MMC, leading to an

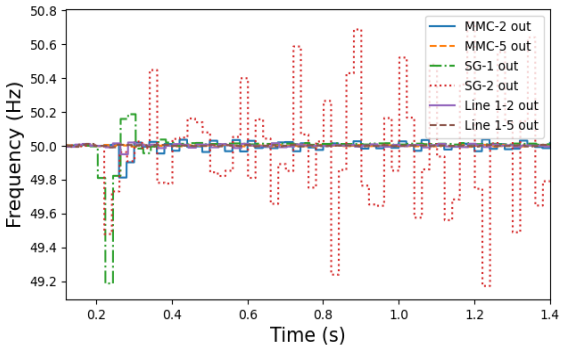

Fig. 5. Frequency response at bus 7 for different outages

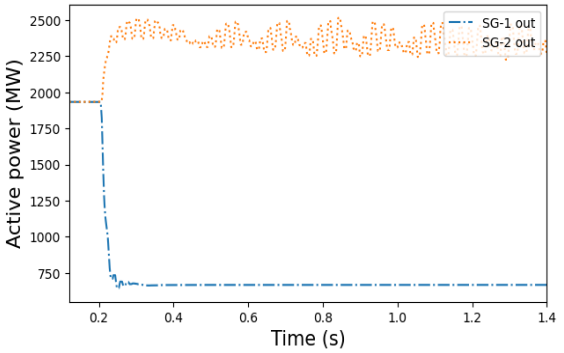

Fig. 6. Active power flow in line 6-7 for different outages

immediate drop of the DC voltage to zero. However, for a line-to-ground fault at the converter, only the voltage of the faulted line would drop to zero, enabling the continued utilization of half of the transport capacity via the other polarity. Additionally, Fig. 7 indicates that the impact of line faults diminishes with increasing distance from the converter.

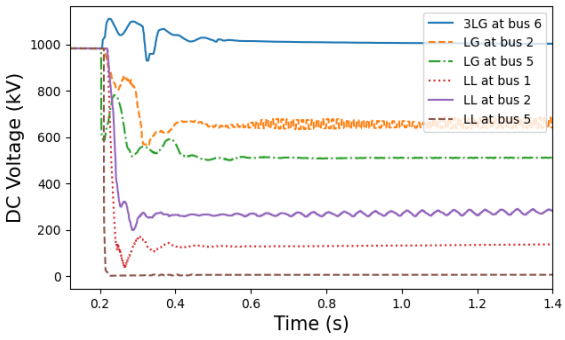

Fig. 7. DC voltage response for different short circuit events

Table V summarizes the calculated performance metrics for both outage and short circuit disturbances. In general, the values of RoCoF and RoCoV provide useful insights into the relative severity of the disturbances. However, there are instances where these metrics may not accurately reflect the perceived impact. For instance, the RoCoV value for the loss of SG-2 is unexpectedly low compared to other disturbances. This discrepancy is evident from Fig. 2, which demonstrates that the voltage dip caused by SG-2 is significantly more pronounced than that of other outages. Similarly, the RoCoF values for the outages of SG-1 and SG-2 are relatively close, despite the more pronounced frequency excursion observed for SG-2 in Fig. 5. This suggests that RoCoF may not capture the full extent of the frequency disturbance induced by SG-2.

The same is observed when comparing the values of RoCoF for the outages of SG-1 and SG-2. The determined values are relatively close. Comparing the responses in Fig. 5, it is observed that the response for an outage of SG-2 has more influence on the response, and should have resulted in a higher RoCoF over time.

TABLE V
CALCULATED PERFORMANCE METRICS

Outage	RoCoF (Hz/s)	RoCoV (kV/s)	Short Circuit	RoCoV (kV/s)
MMC-2	0.001136	112.7	3LG ACF at bus 6	504.8
MMC-5	0.4470	755.8	LG DCF at bus 1	1667
SG-1	1.619	150.1	LG DCF at bus 2	1393
SG-2	1.880	745.4	LL DCF at bus 1	3426
Line 1-2	0.01154	27.66	LL DCF at bus 2	2902
Line 1-5	0.5087	767.6	LL DCF at bus 5	3912

B. Parametric Sensitivity Analyses

To assess the sensitivity of the system's dynamic response to different control parameter configurations, four types of parameters within the outer loop of each MMC's controller are varied over a broad range: Proportional Gain (PG), Integral Gain (IG), Dead-Band Slope(DBS), and Dead-Band Width(DBW). The considered parameter ranges are summarized in Table VI.

TABLE VI
SUMMARY OF CONTROL PARAMETER SETTINGS

Parameter	Values	Control loops
Proportional Gain (PG)	0, 1, 5, 10, 25, 50, 75, 100	Active power DC voltage
Integral Gain (IG)	1 s, 0,2 s, 0,1 s, 0,04 s, 0,02 s, 0,0133 s, 0,01 s	Active power DC voltage
Dead-Band Gain (DBG)	0, 1, 5, 10, 25, 50, 75, 100	Active power
Dead-Band Width (DBW)	0%, 1%, 5%, 10%, 15%, 20%, 25%, 50%	Active power

The previous section identified line-to-line short circuits at the converter as the most severe DC side disturbance, resulting in an immediate drop of the DC voltage to zero. The parametric sensitivity analyses revealed that adjusting the control parameters has no impact on the response to this disturbance. The most influential AC side disturbance is the outage of SG-2, causing significant oscillations in the DC voltage. To address this issue, two potential solutions are investigated: assigning the DC voltage control to MMC-5 or implementing a distributed DC voltage control strategy with both MMC-2 and MMC-5 actively maintaining DC voltage stability..

Figure 8 illustrates the DC voltage response after the outage of SG-2 when MMC-2 is responsible for DC voltage control. Removing the dead-band control block led to the most pronounced oscillations and voltage excursions. Conversely, setting the dead-band width to 0% and increasing the dead-band slope effectively mitigated these undesirable effects.

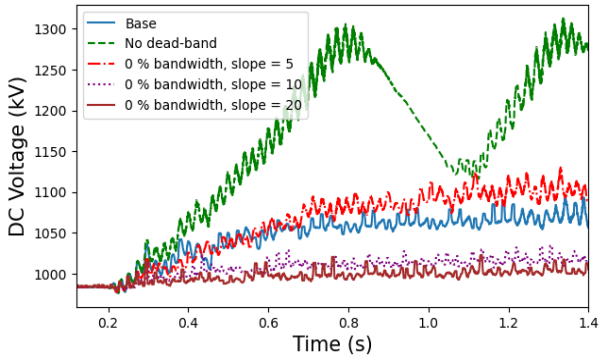

Fig. 8. DC voltage response for SG-2 outage with MMC-2 as DC voltage control

Figure 9 shows the DC voltage response for the outage of SG-2 with MMC-5 in being the responsible converter for DC voltage control. A similar trend is observed, with the dead-band control block significantly reduces oscillations and voltage excursions. Moreover, assigning DC voltage control to MMC-5 generally resulted in better dynamic performance compared to the base case (MMC-2 control).

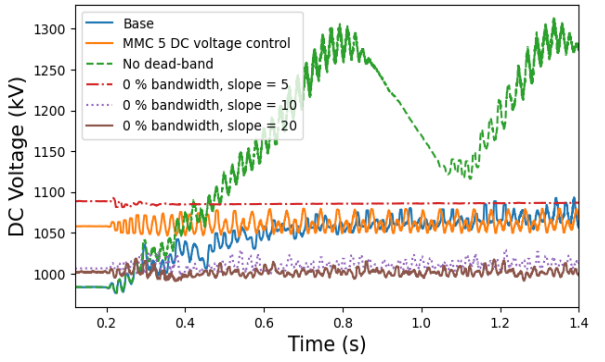

Fig. 9. DC voltage response for SG-2 outage with MMC-5 as DC voltage control

The remainder of this section examines the impact of control parameter tuning on the second-most influential AC side disturbance, a 3-lines-to-ground short circuit at bus 6, as depicted in Fig. 7 and Table V. The results revealed that adjusting the control parameters had a limited impact on mitigating the voltage excursions induced by this disturbance. However, a dead-band control block with a zero width and a high slope still provided some benefit.

1) Proportional gain and Dead-band parameters: The sensitivity of the DC voltage response to different control parameter configurations is investigated. The focus is on the PG K_p of the DC voltage control and active power control, as well as the dead-band parameters (bandwidth and slope).

The PG K_p of the DC voltage control has a significant impact on the initial overshoot and settling time of the system. A lower value of K_p DC leads to a lower overshoot and faster settling time, while a higher value results in larger oscillations as depicted in Fig. 10. The fastest settling time is achieved with K_p set to 5.

In contrast, adjusting the PG of the active power control K_p PWR has a detrimental effect on the dynamic performance of the system. Regardless of the setting, K_p PWR introduces large oscillations, which necessitate the use of a dead-band block in the active power control loop (cf. Table IV).

The DC voltage responses in Fig. 12 demonstrate that both DB parameters influence the overshoot and settling time of the system. Increasing or decreasing the bandwidth has a negative impact, the increase causes higher overshoot and slower settling time. On the other hand, decreasing the bandwidth can lead to instability, particularly with a very small value. In contrast, removing the bandwidth has a positive effect, resulting in lower overshoot and faster settling time. However, a steep slope can lead to large oscillations.

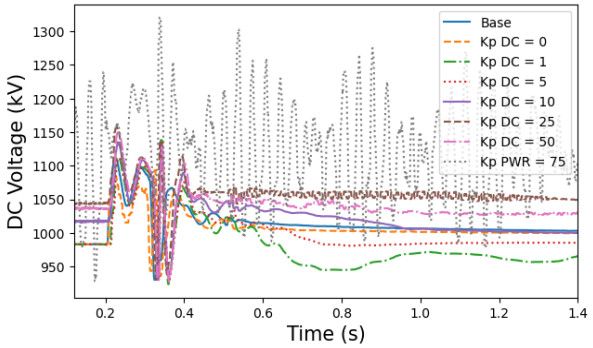

Fig. 10. DC voltage response for different proportional gains

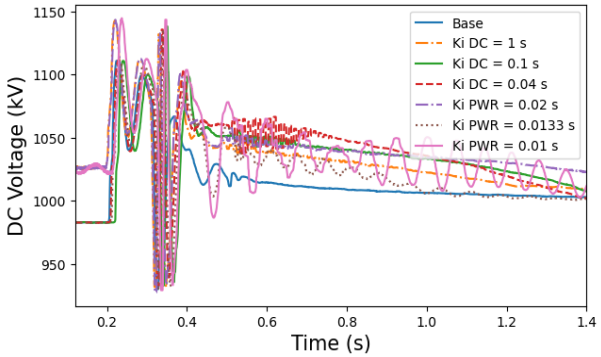

Fig. 11. DC voltage response for different integral gains

As discussed earlier in Section IV-A, the RoCoV performance metric proves inadequate for assessing the dynamic behavior of the system in the presence of oscillatory responses. To address this limitation, an alternative metric is employed to gauge the impact of control parameters. This metric calculates the total area corresponding to deviations in DC voltage from its nominal value.

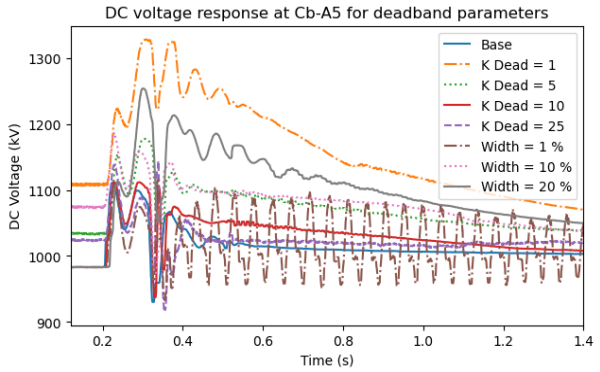

Fig. 12. DC voltage response for different dead-band parameters

The modified metric RoCoV effectively captures both overshoot and settling time, as detailed in Table VII. The results reveal that the optimal combination of control parameters occurs when K_p DC is set to 5 and K_i PWR is set to 0.04 s, resulting in the smallest area and, consequently, the best dynamic performance. This configuration further substantiates the positive influence of eliminating the dead-band bandwidth.

TABLE VII
CALCULATED PERFORMANCE METRICS

Proportional gain K_p	**DC voltage (bus 5) (kV*s)**	**Integral gain K_i**	**DC voltage (bus 5) (kV*s)**
Base	52.08	Base	52.08
K_p DC = 0	41.40	K_i DC = 1	34.57
K_p DC = 1	45.12	K_i DC = 0.2	30.72
K_p DC = 5	27.73	K_i DC = 0.1	29.98
K_p DC = 10	35.84	K_i PWR = 0.04	26.47
K_p DC = 25	36.31	K_i PWR= 0.002	36.26
K_p DC = 50	32.15	K_i PWR= 0.0133	61.56
K_p PWR = 75	212.9	K_i PWR= 0.01	35.88
Slope = 5	120.5	Bandwidth = 0 %	52.08
Slope = 25	18.06	Bandwidth = 1 %	65.43
Slope = 50	62.26	Bandwidth = 10 %	57.99

V. CONCLUSION

This paper has investigated the dynamic performance of an MTDC interconnected offshore-onshore system subjected to various disturbances. The study utilizes RoCoF for AC side evaluation and a modified RoCoV for DC side assessment. The performance metrics effectively capture the qualitative impact of disturbances in most cases, except for oscillatory responses. Visual inspection of DC voltage time responses reveals that a line-to-line short circuit near the converter is the most impactful DC side disturbance, unaffected by adjustments in control parameters. Future studies should explore alternative DC voltage control forms and their interaction with protection mechanisms.

A power plant outage near the controlling converter emerges as the most impactful AC side disturbance, causing oscillations and DC voltage excursions. Parametric sensitivity analysis indicates that distributed DC voltage control, with optimally tuned dead-band control blocks (dead-band removal and converter properties dependent slope), effectively mitigates this outage's impact .The second-most influential AC side disturbance is analyzed using the total area of DC voltage deviation from nominal value. The results indicate that relatively low proportional gain (K_p around 5 p.u.)and integral gain (K_i around 0.04 s) entail the smallest computed area. These settings lead to reduced DC excursions and faster settling. Additionally, a bandwidth control block with zero width and a steep slope further enhances stability by reducing the area.

REFERENCES

[1] A. A. Bajwa, "Enhancing Power System Resilience Leveraging Microgrids: A Review", *Journal of Renewable and Sustainable Energy*, 2019.

[2] B. Ti and G. Li and M. Zhou and J. Wang, "Resilience Assessment and Improvement for Cyber-Physical Power Systems under Typhoon Disasters",*IEEE Transactions on Smart Grid*, 2022.

[3] P. Gasser and P. Lustenberger and M. Cinelli,"A Review on Resilience Assessment of Energy Systems", *Sustainable and Resilient Infrastructure*, 2021.

[4] M. Muniappan, "A Comprehensive Review of DC fault Protection Methods in HVDC Transmission Systems", *Protection and Control of Modern Power Systems*, 2021.

[5] R. H. Wickramasinghe and G. Konstantinou, "Interoperability of Modular VSC Topologies in Multi-converter Multiterminal DC Systems", *Electric Power Systems Research* , 2021.

[6] M. Liu and J. Chen and F. Milano, "On-line Inertia Estimation for Synchronous and Non-Synchronous Devices, *IEEE Transactions on Power Systems*, 2020.

[7] M. Sun and G. Xie and Y. Liu and Y. Min, "Study on the Necessity and Role of Inertia in Power System Frequency Response", *in Proc. IEEE 4th Conference on Energy Internet and Energy System Integration (EI2)*, 2020.

[8] X. Deng and R. Mo and P. Wang and J. Chen and D. Nan and M. Liu, "Review of RoCoF Estimation Techniques for Low-Inertia Power Systems", *Energies*, 2023.

[9] T. Bavsakarad and N. Holjevac and I. Kuzle, "Rocof Importance in Electric Power Systems with High Renewables Share: A Simulation Case for Croatia", *IET*, 2021.

[10] L. Dewangan and H. Bahirat, "Comparison of HVDC grid control strategies", *In Proc. IEEE PES Asia-Pacific Power and Energy Engineering Conference (APPEEC)*, 2017.

[11] H. S. Salama and I. Vokony, "Voltage stability indices–A comparison and a review", *Computers & Electrical Engineering*, 2022.

[12] M. J. Pereze-Molina, P. Eguia and M. Larruskain and G. Buigues, "Non-unit ROCOV Scheme for Protection of Multi-terminal HVDC Systems", *In Proc. 22nd European Conference on Power Electronics and Applications (EPE'20 ECCE Europe)*, 2020.

[13] J. Sneath and A. D. Rajapakse, "Fault Detection and Interruption in an Earthed HVDC Grid Using ROCOV and Hybrid DC Breakers", *IEEE Transactions on Power Delivery*, 2014.

[14] RTDS Technologies, "RSCAD®FX Introductory Tutorial", Winnipeg Canada, 2020.

[15] RTDS Technologies, "RSCAD® FX NovaCor", Winnipeg Canada, https://www.rtds.com/wp-content/uploads/2019/08/NovaCor.pdf, 2019.

[16] CIGRE B4.72, "DC grid benchmark models for system studies", https://e-cigre.org/publication/804-dc-grid-benchmark-models-for-system-studies , 2020.

[17] RTDS Technologies, "MMC5 Converter Model", Winnipeg Canada, 2020.

[18] CIGRE B4.57, "Guide for the Development of Models for HVDC Converters in a HVDC Grid", https://e-cigre.org/publication/604-guide-for-the-development-of-models-for-hvdc-converters-in-a-hvdc-grid , 2014.